Received: 20 April 2023 | Accepted: 15 August 2023

DOI: 10.1111/1462-2920.16501

RESEARCH ARTICLE

ENVIRONMENTAL MICROBIOLOGY Applied Microbiology International

Anaerobic methanotrophy is stimulated by graphene oxide in a brackish urban canal sediment

Koen A. J. Pelsma[1,2] | **Niels A. G. M. van Helmond**[1,3] | **Wytze K. Lenstra**[1,2,3] | **Thomas Röckmann**[4] | **Mike S. M. Jetten**[1,2] | **Caroline P. Slomp**[1,2,3] | **Cornelia U. Welte**[1]

[1]Department of Microbiology, Radboud Institute for Biological and Environmental Sciences, Radboud University, Nijmegen, The Netherlands

[2]Netherlands Earth System Science Centre, Utrecht University, Utrecht, The Netherlands

[3]Department of Earth Sciences, Faculty of Geosciences, Utrecht University, Utrecht, The Netherlands

[4]Institute for Marine and Atmospheric Research Utrecht, Utrecht University, Utrecht, The Netherlands

Correspondence
Cornelia U. Welte, Department of Microbiology, Radboud Institute for Biological and Environmental Sciences, Radboud University, Heyendaalseweg 135, 6525AJ Nijmegen, The Netherlands.
Email: c.welte@science.ru.nl

Funding information
H2020 European Research Council, Grant/Award Number: 854088; Nederlandse Organisatie voor Wetenschappelijk Onderzoek, Grant/Award Numbers: 024002001, 024002002

Abstract

Anthropogenic activities are influencing aquatic environments through increased chemical pollution and thus are greatly affecting the biogeochemical cycling of elements. This has increased greenhouse gas emissions, particularly methane, from lakes, wetlands, and canals. Most of the methane produced in anoxic sediments is converted into carbon dioxide by methanotrophs before it reaches the atmosphere. Anaerobic oxidation of methane requires an electron acceptor such as sulphate, nitrate, or metal oxides. Here, we explore the anaerobic methanotrophy in sediments of three urban canals in Amsterdam, covering a gradient from freshwater to brackish conditions. Biogeochemical analysis showed the presence of a shallow sulphate–methane transition zone in sediments of the most brackish canal, suggesting that sulphate could be a relevant electron acceptor for anaerobic methanotrophy in this setting. However, sediment incubations amended with sulphate or iron oxides (ferrihydrite) did not lead to detectable rates of methanotrophy. Despite the presence of known nitrate-dependent anaerobic methanotrophs (*Methanoperedenaceae*), no nitrate-driven methanotrophy was observed in any of the investigated sediments either. Interestingly, graphene oxide stimulated anaerobic methanotrophy in incubations of brackish canal sediment, possibly catalysed by anaerobic methanotrophs of the ANME-2a/b clade. We propose that natural organic matter serving as electron acceptor drives anaerobic methanotrophy in brackish sediments.

INTRODUCTION

Freshwater and estuarine environments are increasingly recognized as potential hotspots of greenhouse gas emissions, with the rate of methane (CH_4) release from these ecosystems being of particular interest (Peacock et al., 2021; Rosentreter et al., 2021; Saunois et al., 2020). Atmospheric CH_4 has a global warming potential that is 86 times higher (20-year timescale) than carbon dioxide (CO_2; Dean et al., 2018; Myhre et al., 2013; Nisbet et al., 2019). Sources of atmospheric CH_4 are often biological, such as estuaries, lakes, and wetlands (Rosentreter et al., 2021). Like estuaries, urbanised waters are putative hotspots of CH_4 emissions as they are heavily influenced by anthropogenic nutrient input (Connor et al., 2014; van Bergen et al., 2019) and not many studies have been performed on urban waters to date (Hu et al., 2022; Pelsma et al., 2022).

Relatively high CH_4 concentrations and emissions from fresh and estuarine waters have been reported for several riverine systems in Europe (Alshboul et al., 2016; Borges et al., 2018; Herrero Ortega et al., 2019; Marescaux et al., 2018), China (Wang

et al., 2018; Wang et al., 2021), and the United States (Brigham et al., 2019). A recent study of built canals in urban and agricultural environments showed that CH_4 emissions from these systems can be as high as those from tropical wetlands, and even higher than those from freshwater lakes (Peacock et al., 2021). Most studies find a positive correlation between temperature and concentrations of CH_4. However, other environmental parameters, such as nutrient and oxygen concentrations, are not always correlated to increased CH_4 production or emissions (Herrero Ortega et al., 2019) illustrating that we do not yet fully understand how environmental conditions influence CH_4 emissions (Gessner et al., 2014).

Methane is produced in anoxic sediments and before it reaches the atmosphere, a large part of the CH_4 is removed by the activity of methanotrophic bacteria and archaea, in either the sediment or overlying water (Conrad, 2009). Oxygen is used as a terminal electron acceptor for bacterial methanotrophs and is dominant in oxic environments. In anoxic environments, the oxidation of CH_4 occurs mainly by methanotrophic archaea. Syntrophic consortia of methanotrophic archaea and sulphate (SO_4^{2-})-reducing bacteria (SRB) use SO_4^{2-} as an electron acceptor and consume 7%–25% of globally produced CH_4 (Gao et al., 2022; Knittel & Boetius, 2009). This process occurs in the sulphate–methane transition zone (SMTZ) of marine sediments (Reeburgh, 2007). SO_4^{2-}-mediated anaerobic oxidation of methane (AOM) is thought to play a less important role in brackish environments due to the lower availability of SO_4^{2-}compared with marine systems. Anaerobic methanotrophs may use other electron acceptors as well, like nitrate (NO_3^-), nitrite (NO_2^-), Fe(III), and Mn(IV) (Cai et al., 2018; Ettwig et al., 2016; Haroon et al., 2013; Leu et al., 2020; Raghoebarsing et al., 2006). Moreover, recently also natural organic matter (NOM)-mediated AOM has been observed (Bai et al., 2019; Valenzuela et al., 2017, 2019; Valenzuela & Cervantes, 2021; van Grinsven et al., 2020).

Recent studies highlighted the presence of AOM in several natural and engineered ecosystems (Fan et al., 2020; Martinez-Cruz et al., 2018; Pelsma et al., 2022; Shen et al., 2019; Valenzuela et al., 2019). A recent study of the CH_4-cycling microbial community in the canals of Amsterdam showed the presence of anaerobic methanotrophic (ANME) *Methanoperedenaceae* in the sediment leading to the question if anaerobic methanotrophy could take place, and which potential terminal electron acceptors might be used (Pelsma et al., 2022). In this study, we investigated which electron acceptors are available through biogeochemical characterization and microcosm incubations of Amsterdam canal sediments. In addition, we aimed to identify the key microbes involved in AOM. Since a salinity gradient exists within Amsterdam, we sampled three different salinities as this could impact the availability of electron acceptors such as SO_4^{2-}.

EXPERIMENTAL PROCEDURES

Study sites

The canals of Amsterdam are subject to an influx of brackish water from the IJ and the North Sea Canal. Salinity is monitored by the Department of Waterways and Public Works of the Dutch government (Rijkswaterstaat). All corresponding data are publicly available on their website (https://waterinfo.rws.nl). To capture as much microbial diversity as possible within the same urban canal network, we chose three sites across a gradient in salinity, from fresh water in the Amstel River (salinity of 1), an intermediate brackish site, the Zoutkeetsgracht (salinity of 4) to the most brackish water in the Dijksgracht (salinity of 5–6; Figure 1 and Table 1). Furthermore, we hypothesised that different salinities (or more or less marine influence) could alter the electron acceptors presence in the sediment. For example, higher salinities could have higher SO_4^{2-} penetration into the sediment, whereas NO_3^- might be more available in freshwater canals.

Sampling strategy

Sampling of water and sediment was carried out from 17 to 19 May 2021. *In situ* water parameters (salinity, dissolved oxygen, temperature) were measured using a ProDSS Multiparameter Digital Water Quality Meter (YSI Inc., Yellow Springs, OH, USA). Surface water was collected using an acid-washed 10 L carboy. Subsamples were taken for the determination of dissolved CH_4, ammonium (NH_4^+), NO_3^-, dissolved iron and manganese, and SO_4^{2-} (stored at 4°C; Supplementary Methods S1).

Per study site, six sediment cores were taken with a UWITEC gravity corer (UWITEC GmbH, Mondsee, Austria) using transparent PVC core liners of 60 cm in length and an inner diameter of 6 cm. Presence of filter feeders hampered the gravity coring at the Amstel River and Zoutkeetsgracht sites, limiting the coring depth. Samples for bottom and pore water CH_4 and its isotopic composition were collected directly after core retrieval with 10 mL cut-off syringes via pre-drilled holes at 2.5 cm depth intervals that were covered with tape prior to coring. No porewater CH_4 data could be collected for the Amstel due to equipment failure. The remaining five sediment cores were brought to the laboratory at Utrecht University and processed the same day. The second core was sliced in a glove bag under a nitrogen atmosphere. First, two bottom water samples were taken from the overlying water. The core was then sliced at a depth resolution of 1 cm into 50 mL centrifuge tubes. Sample resolution was maintained at 1 cm for the first 10 cm, after which the resolution was lowered to one sample per 2 cm. Details on core handling and pore water extraction are described in the

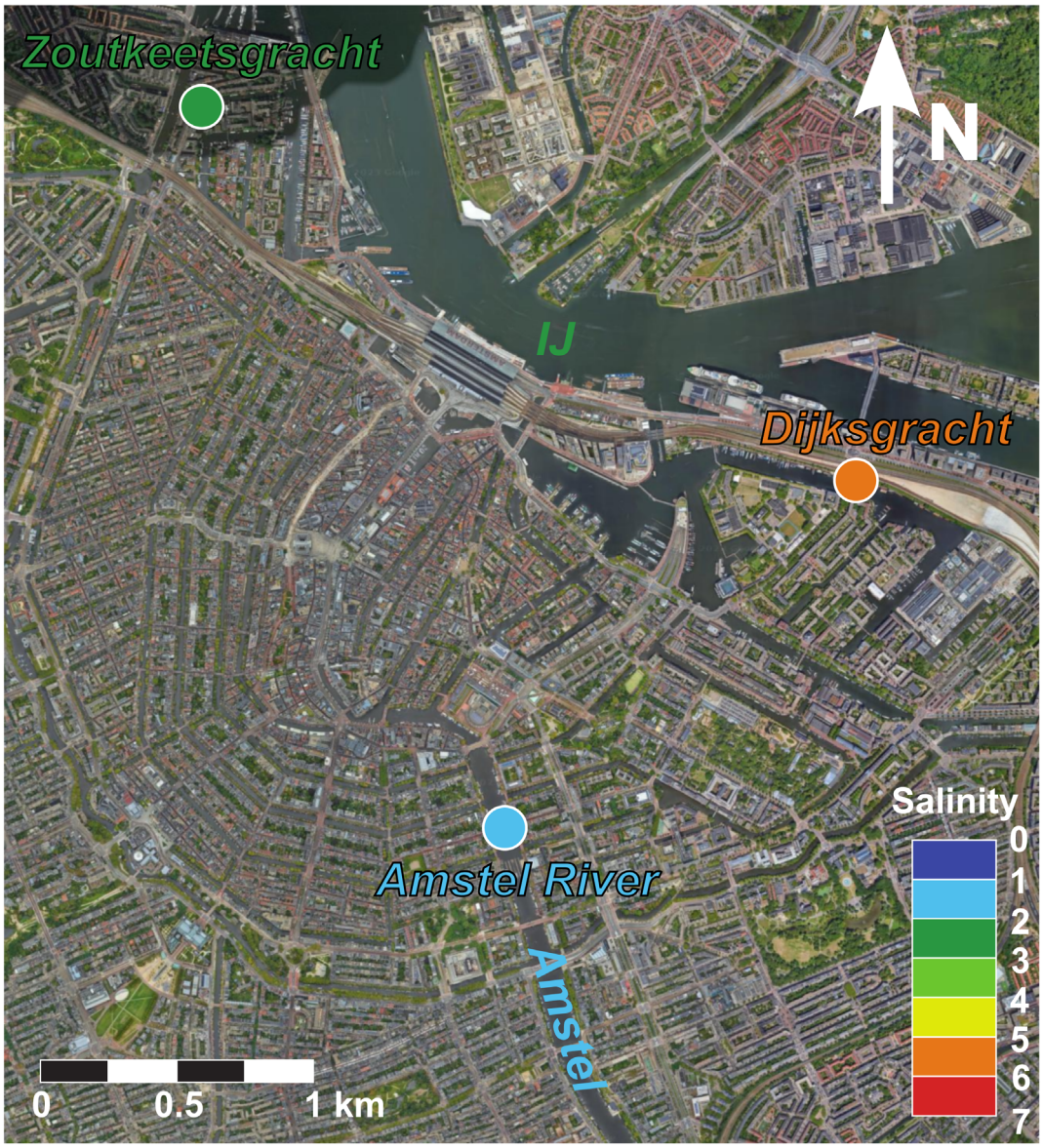

FIGURE 1 City centre of Amsterdam with the study sites indicated by circles. Colour coding of the study sites is based on the ambient salinity at the time of sampling (Table 1). Map data were obtained from Google Earth (Google, n.d.).

Supplementary Methods S1. For AOM microcosm incubations, three sediment cores were sliced with five intervals (0–2, 2–5, 5–10, 10–15, and 20–25 cm) and collected in sterile plastic bags, stored anoxically in nitrogen-filled aluminium bags at 4°C and brought to the laboratory at Radboud University where the slices were transferred into an anaerobic hood for further processing.

Greenhouse gas flux measurements

Diffusive fluxes of CO_2 and CH_4 were measured in the field with a floating chamber and a LI-COR 7810 $CH_4/CO_2/H_2O$ Trace Gas analyser (LI-COR, Inc., Lincoln, NE, USA). At least three replications at each site were measured and the linear increase in greenhouse gas concentration (ppm or ppb per second) was used to calculate the flux (mmol m^{-2} day^{-1}). Flux data analysis was automated in Python 3.6 (https://python.org) by filtering the data using a Savitsky–Golay filter and using the filtered data to find the peaks that indicated the end of a flux measurement. Linear regression was performed on the peak point and a data point that lay 2 min prior. Conversion of the increase in mole fraction (ppb) to a flux rate of CO_2 and CH_4 in mmol m^{-2} day^{-1} was done with Equation (1)

$$F_{CH4} = \frac{\Delta ppb}{\Delta t} \frac{PM_W V_{Chamber}}{RTArea_{Chamber} 1000} \quad (1)$$

TABLE 1 *In situ* water column characteristics at two different depths (surface and bottom).

	Amstel River	Zoutkeetsgracht	Dijksgracht
Coordinates (DD.ddddd)	N 52.36361	N 52.38818	N 52.37505
	E 4.90238	E 4.88565	E 4.921396
Surface water			
DO (%)	98.2	100	100
Water temperature (°C)	16	14	14.5
Salinity	1.28	2.69	2.28
Air temperature (°C)	11.2	12.9	13.6
CH_4 flux (mmol m^{-2} day^{-1})	0.21 ± 0.06	0.44 ± 0.04	0.17 ± 0.09
CO_2 flux (mmol m^{-2} day^{-1})	48.4 ± 6.4	N.D.	N.D.
Bottom water			
DO (%)	98.2	100	12.7
Water temperature (°C)	16	13.7	12
Salinity	1.28	3.8	5.48
Water depth (m)	4	2	4.5
Macrofauna	Yes, *Corbicula*	Yes, *Anodonta*	No

Abbreviations: DO, dissolved oxygen; N.D., not detected.

Water column and pore water analysis

Dissolved concentrations CH_4 of the canal water and pore water were measured, after addition of a nitrogen headspace (5 mL for the water column samples and 10 mL for the pore water samples) and equilibration of the gas and water phase for a week, with a Thermo Finnigan (Thermo Fisher Scientific, USA) trace gas chromatograph equipped with a flame ionization detector at Utrecht University. A separate measurement was done on a Hewlett Packard 5890 Series II (Agilent Technologies, USA) trace gas chromatograph equipped with a Porapak Q-column (100/120 mesh) and a flame ionisation detector at Radboud University (pore water samples) by triplicate injections of 50 μL. Stable isotope analysis of porewater-dissolved CH_4 was performed at the Institute for Marine and Atmospheric Research at Utrecht University (see Supplementary Methods S1 for details). Dissolved sulphide, SO_4^{2-}, NH_4^+, NO_3^-, NO_2^-, Fe, and Mn were measured using spectrophotometric methods or ICP-OES as described in the Supplementary Methods S1.

Sediment analysis

Sediment samples taken for the determination of porosity were weighed, oven-dried (1 week at 60°C) and weighed again to determine the water content. Sediment porosity was then calculated assuming a solid phase density of 2.65 g cm^{-3} (Burdige, 2007). Sediment samples from the anoxic core were freeze-dried, powdered, and homogenized in a nitrogen-filled glovebox, using an agate mortar and pestle. Fe-carbonates, Fe-monosulfides, and easily reducible Fe-oxides were extracted from anoxic core samples using 1 M HCl. A second anoxic subsample was subjected to a previously described five-step sequential extraction (Lenstra et al., 2021) to separate the different sedimentary forms of Mn and Fe (specifically aiming for the more recalcitrant forms of the latter). Organic carbon and nitrogen were measured using a subsample of sediment that was processed outside of the glovebox on a Fisons Instruments NA 1500 NCS analyser. Details on the extraction procedure and measurements are described in the Supplementary Methods S1.

Sediment incubations

To prepare the sediment slurries for the microcosm incubations, canal water was filtered over a 0.22 μm polyethersulfone filter. Subsequently, the filtered canal water was made anoxic through a vacuum-gassing cycle with N_2 for a total of 5 cycles. Within an anaerobic hood under N_2 atmosphere, sediment core slices were slurried 1:1 w/w with the filtered and anoxic canal water using a scale. To set up the microcosm incubations, autoclaved 120 mL serum bottles were transferred to the anaerobic hood. Each microcosm incubation contained 25 mL of this slurried sediment. All bottles were closed off with red butyl rubber stoppers and sealed with aluminium crimp caps inside the anaerobic hood to minimise oxygen exposure as much as possible. Before the addition of CH_4 or electron acceptors, the pressure was normalized to ~0.3 bar N_2 atmosphere

using an eight-way gas exchanging valve. Pressures were checked with a digital pressure meter (GMH 3111, GHM Messtechnik GmbH, Germany).

Endogenic production of CH_4 from the sediment was measured for each slurry by following the increase in CH_4 concentration for 10 days (Figure S1). A positive control was taken along by adding 2 mM sodium acetate to the slurries. Killed controls were made by autoclaving the sediment slurries for 20 min at 120°C. Microcosm incubation for AOM was started by adding 2.5 mL of $^{13}CH_4$ using a syringe to the headspace (total headspace volume of 95 mL) of each bottle, resulting in an approximate headspace concentration of 2% $^{13}CH_4$. Care was taken not to drop the overpressure in the bottles when using the syringe. This gives a dissolved CH_4 concentration of 37 μM according to Henry's Law. The effect of electron acceptors was tested by adding 4 mM NO_3^-, 4 mM SO_4^{2-}, 10 mM ferrihydrite, and 200 mg L^{-1} graphene oxide (GO) to their respective bottles. GO was chosen as a NOM analogue because it consists of a graphene sheet with edge group hydroxyls, epoxides, carbonyls, quinones, and carboxylic acids. The concentration of 200 mg L^{-1} was chosen as this was proven to be adequate for an anammox enrichment culture and an ANME enrichment culture (Berger et al., 2021; Shaw et al., 2020). Stock solutions were made anoxic prior to the start of the experiments using chemicals bought from Sigma-Aldrich (Merck KGaA, Germany). Syringes were used to inject electron acceptors into the microcosm incubations. Before every injection, syringes were flushed with 100% N_2 three times their volume. Control incubations were carried out without the addition of CH_4 to the headspace and without the addition of any electron acceptors. The amount of replicates and treatments are summarised in Tables S1 and S2. To determine the rate of AOM, the enrichment of $^{13}CO_2$ was measured using a gas chromatograph coupled to a mass spectrometer (6890 Series GC coupled to a 5975C MS, Agilent Technologies). Enrichment of $^{13}CO_2$ was calculated by comparing it to the Vienna Pee Dee Belemnite (VPDB) standard using the formula:

$$\delta^{13}CO_2 = \left(\frac{\left[{}^{13}CO_2 \right] \Big/ \left[{}^{12}CO_2 \right]}{\left(R_{sample} \right)} - 1 \right) \times 1000$$

where R_{sample} was 0.01123720. The rate was calculated from data points of the first 10 days as the slope of a linear least squares regression of each replicate separately (data in Figure S2). Treatments were averaged after normalization to g_{DW}. All anaerobic incubations were performed at 20°C and in the dark, while shaking on a plateau at 105 rpm.

DNA isolation and 16S rRNA gene amplicon sequencing

Microbial community profiling was done by sequencing 16S rRNA gene amplicons using DNA template from core slices that were taken on the day of sampling and stored at −80°C. Filters were stored at −20°C until further processing. DNA was isolated for all samples using the DNeasy PowerSoil DNA Isolation kit according to the manufacturer's instructions (Qiagen, Venlo, The Netherlands), with the alteration that the PowerBead tubes were bead-beated on a TissueLyser LT (Qiagen) for 10 min at 50 Hz and the DNA was eluted using DEPC-treated water. Eluted DNA was stored at 4°C until sequencing. 16S rRNA gene amplicon sequencing was done by Macrogen (Macrogen Inc., Seoul, Korea) using the Illumina MiSeq Next Generation Sequencing platform. Paired-end libraries were constructed using the Illumina Herculase II Fusion DNA Polymerase Nextera XT Index Kit V2 (Illumina, Eindhoven, The Netherlands). Primers used for bacterial amplification were Bac341F (5′-CCTACGGGNGGCWGCAG-3′; Herlemann et al., 2011) and Bac806R (5′-GGACTACHVGGGTWTCTAAT-3′; Caporaso et al., 2012; Figure S5). Archaeal amplification was performed with primers Arch349F (5′-GYGCASCAGKCGMGAAW-3′) and Arch806R (5′-GGACTACVSGGGTATCTAAT-3′; Takai & Horikoshi, 2000). The obtained amplicon sequencing reads were processed as outlined in Pelsma et al. (2022). After processing the number of archaeal reads was between 45,000 and 84,000, whereas bacterial sequencing yielded between 30,000 and 70,000 reads. Raw read data for this study was deposited in the European Nucleotide Archive at EMBL-EBI under accession number PRJEB60458 (https://www.ebi.ac.uk/ena/browser/view/PRJEB60458).

RESULTS

Canal water chemistry

The chemical analyses of the water of the three canals confirmed the targeted salinity gradient (Table 1). The water in the Zoutkeetsgracht (medium salinity) and Amstel (freshwater) was fully oxygenated, and the top 5 cm of the sediment contained filter feeders (*Anodonta* sp. and *Corbicula* sp., respectively). Their presence increased the downward transport of oxygen in the sediment, as evident from light-coloured burrows down to a depth of 10 cm. The Dijksgracht (highest salinity) showed much lower oxygen availability at the sediment–water interface with an oxygen saturation level of 12.7%. Flux chamber measurements revealed CH_4 emissions from all three canals (Table 1). The site with the highest CH_4 emission was Zoutkeetsgracht at 0.44 ± 0.04 mmol CH_4 m^{-2} day^{-1}. The Amstel site was

the only site with a net flux of CO_2 to the atmosphere of 48.4 ± 6.4 mmol m^{-2} day^{-1}.

Electron acceptor availability and microbial community analysis

We characterised the sediments at all three study sites for SO_4^{2-}, NO_3^-, reactive Fe and Mn and determined their microbial community composition (Figures 2 and S5). The Amstel River carries freshwater and therefore the Amstel site only had low concentrations of SO_4^{2-} (1 mM) in the porewater. NO_3^- was depleted in the first centimetre. The pore water of the Zoutkeetsgracht sediments, the mildly brackish site, contained up to 4 mM SO_4^{2-}, while its ammonium concentration was lower than that of the Amstel site. Sulphide concentrations in the pore water were low, in line with the limited change of SO_4^{2-} concentration with increasing depth. NO_3^- was depleted after 4 cm at this site. Sediment pore water of the Zoutkeetsgracht contained very little dissolved CH_4 (0.5 μM).

The Dijksgracht canal had the highest bottom water salinity (Table 1) and the highest SO_4^{2-} concentration at 5 mM (Figure 2). The pore water sulphide peaked at 10 cm depth, but absolute concentrations were very low (2 μM). Moreover, the Dijksgracht showed a clear, though shallow SMTZ between 5 and 20 cm core depth and CH_4 concentrations increasing up to 0.5 mM below the SMTZ. Like the Amstel canal, NO_3^- was depleted in the first centimetre.

Reactive Fe and Mn in the sediments of all three canals were dominated by Fe-sulphides and carbonates. Fe(III) and Mn(IV) were also present,

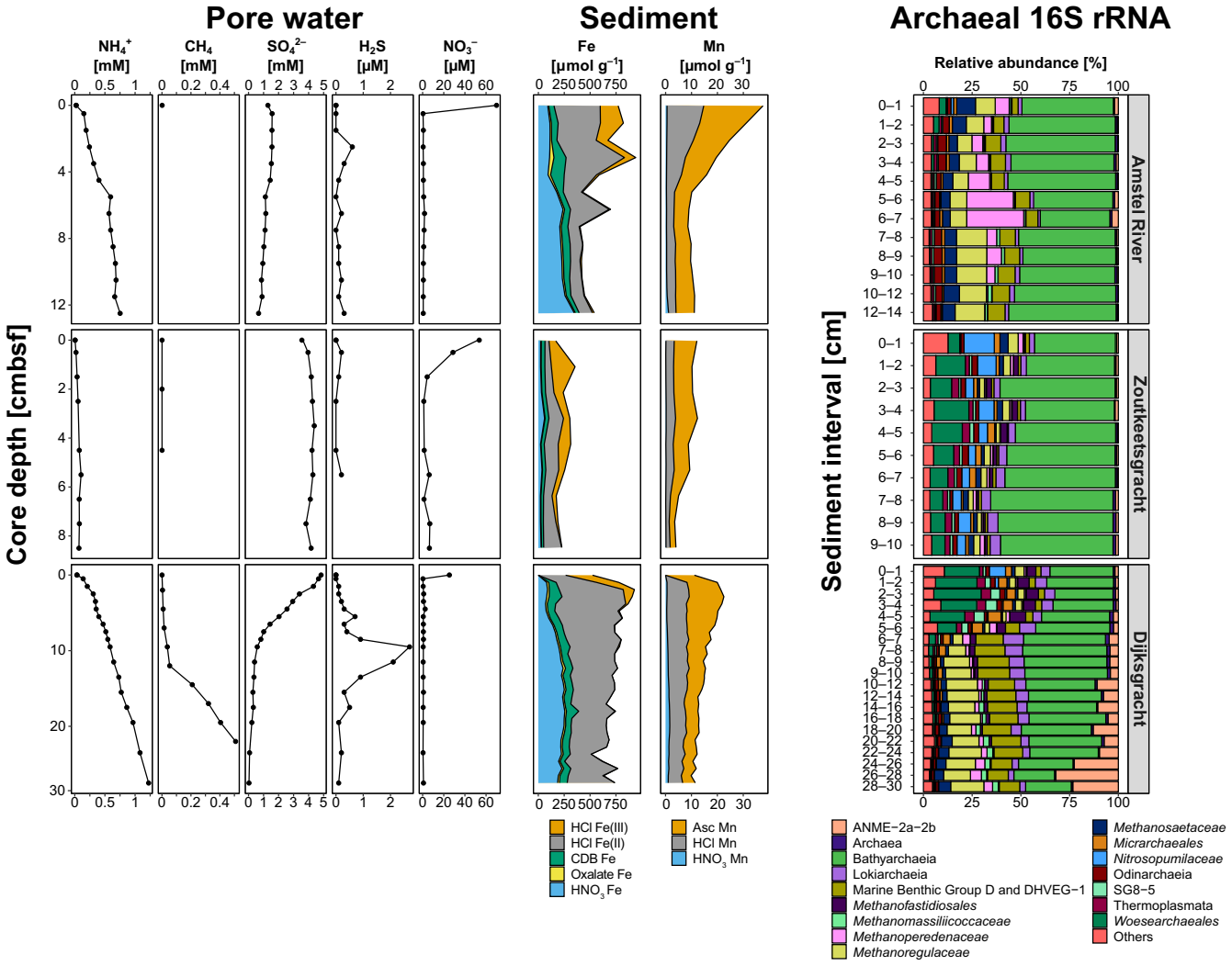

FIGURE 2 Geochemical and microbiological depth profiles of the sediment at three sites in the Amsterdam canals. Please note the different ranges for the x-axis in each column and different y-axis in each row. Asc, ascorbate; HCl, hydrochloric acid; CDB, citrate-dithionite-bicarbonate; HNO_3, nitric acid. Archaeal 16S rRNA gene sequencing results were normalized on merged read count and are displayed in relative abundance per depth interval. All sequences that had <1% abundance were grouped into 'Others'.

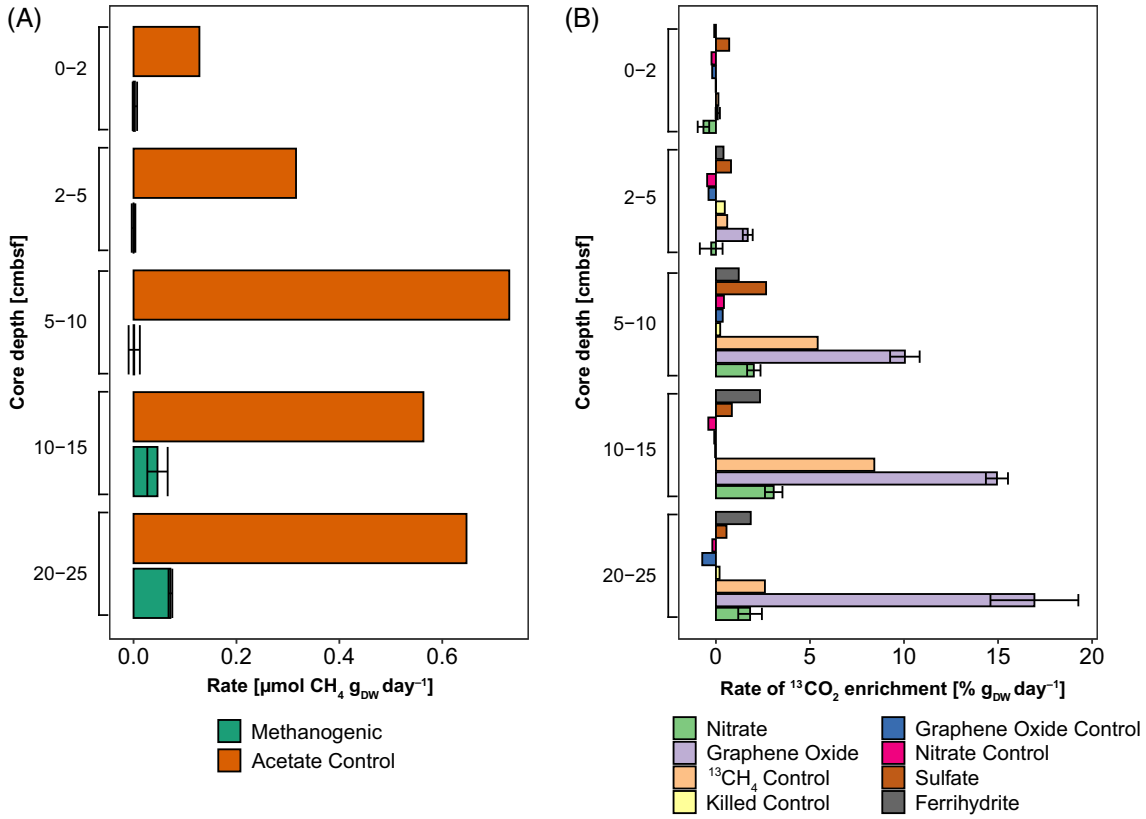

FIGURE 3 Rates of (A) methanogenesis and (B) anaerobic methane oxidation of the Dijksgracht sediment for different electron acceptors. All electron acceptors were added in one dose, except nitrate.

especially in the upper part of the sediment. Surface sediments at the Amstel site, for example, contained around 200 µmol g^{-1} Fe(III). Ascorbate-extracted Mn(IV) amounted to 17 µmol g^{-1}. The Dijksgracht sediment contained most reactive Fe and Mn, 700 and 15 µmol g^{-1} on average, respectively.

The archaeal community of the Amstel site showed a marked increase in the ANME family *Methanoperedenaceae* at 5 cm to 20% relative archaeal abundance. In the sediments of the Zoutkeetsgracht, no ANME families were detected. The most notable CH_4-producing archaea consisted of a combination of *Methanoregulaceae* and *Methanofastidiales*, both methanogenic lineages, at 9% relative archaeal abundance. The ammonium-oxidizing family *Nitrosopumilaceae* comprised 10% of the archaeal community for the first 2 cm of the sediment and persisted to a depth of 10 cm. The Dijksgracht canal showed an increase in ANME2a-2b methanotrophs at depths where NO_3^- and SO_4^{2-} were depleted. Increasing from 5% at 5 cm depth to more than 20% relative abundance at 25 cm depth, these ANME archaea were more abundant than *Methanoperedenaceae*. The methanogenic community of the Dijksgracht canal consisted of the hydrogenotrophic family *Methanoregulaceae*.

Methanogenesis and anaerobic methanotrophy in canal sediments of the Dijksgracht

Results of batch incubations for endogenic CH_4 production showed low production rates for the Zoutkeetsgracht and Amstel River sites (Figures 3A and S3A). Sediments of the Zoutkeetsgracht and Amstel River showed potential for methanogenesis with the addition of acetate (Figure S1A). The Dijksgracht site showed no methanogenic activity in the first 10 cm of the sediment (Figure 3A) and displayed the highest rates in the 20–25 cm depth interval (0.7 µmol CH_4 day^{-1} $g_{DW}{}^{-1}$). The addition of acetate stimulated CH_4 production at all sediment depths (Figure 3A). Furthermore, the isotopic signature of the porewater $^{13}CH_4$ (Figure 4A–D) in the methanogenic zone (15–25 cm core depth) ranged between −61.7‰ and −81.4‰ versus VPDB, while the signature of D ranged between −170.8‰ and −220.3‰ versus Vienna Standard Mean Ocean Water (VSMOW). These signatures correspond to CH_4 production through hydrogenotrophic methanogenesis (Milkov & Etiope, 2018; Whiticar, 1999).

The AOM activity for the brackish Dijksgracht site (Figures 3B and S1) was the highest of all three studied canals. The incubations with NO_3^- showed enrichment

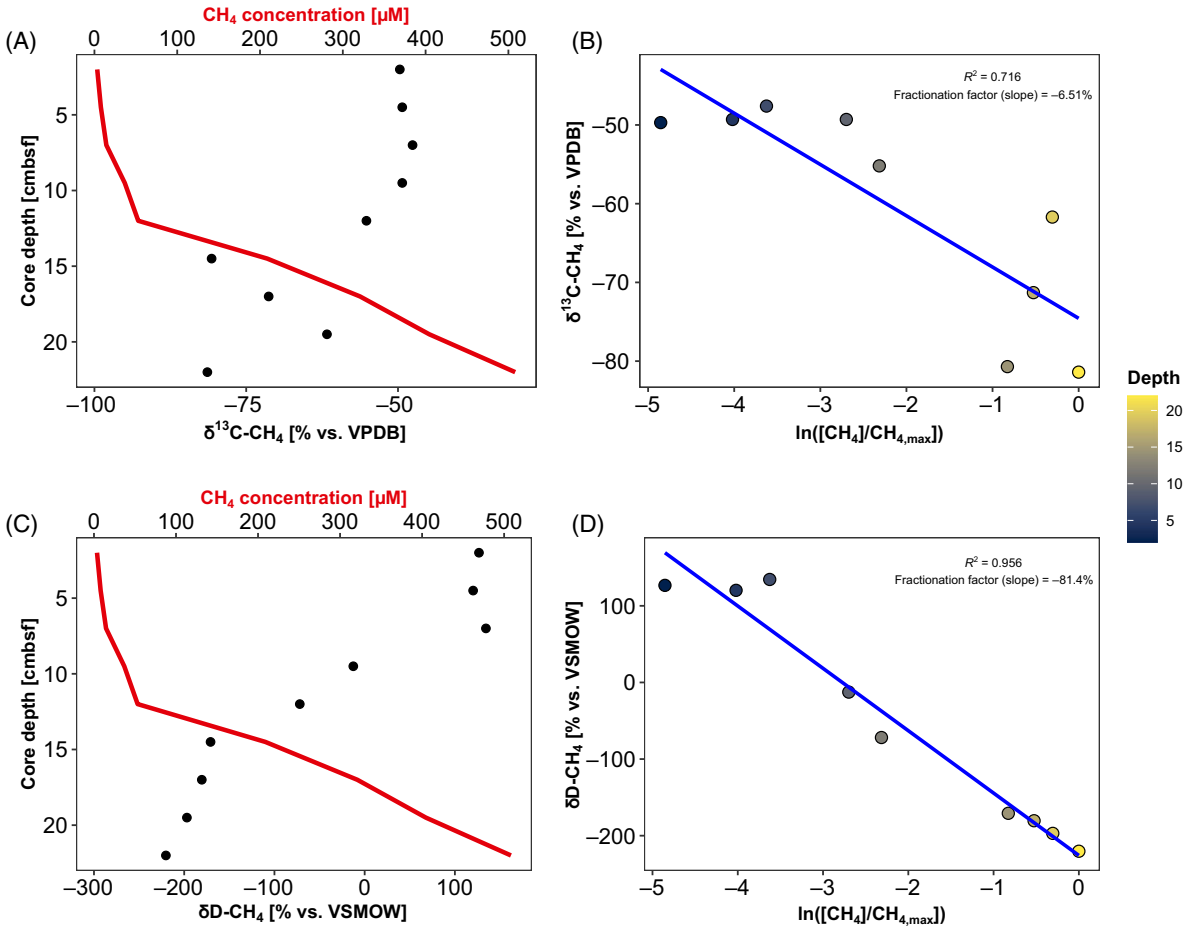

FIGURE 4 Methane isotope analysis of Dijksgracht porewater samples. Panels (A,C) show the isotopic signatures of porewater CH_4 for ^{13}C and D, respectively (black dots), overlain with porewater CH_4 concentrations (red lines). Rayleigh fractionation plots for $^{13}CH_4$ (B) and D (D) were used to calculate the fractionation constants. The blue line is the linear model used for the regression. Each point is coloured based on its core depth in cm below sediment surface. The analytical error bars are smaller than the size of the symbols. We note that the Rayleigh fractionation plot for $\delta^{13}C$ shows unexpectedly large scatter from the fit line, indicating the possible influence of other processes, which could not be identified. VPDB, Vienna Pee Dee Belemnite; VSMOW, Vienna Standard Mean Ocean Water.

of heavy $^{13}CO_2$ after 9 days at a rate of 3.07 ± 0.46‰ day^{-1} $g_{DW}{}^{-1}$ for the 10–15 cm depth interval, with similar rates detected for 5–10 and 20–25 cm (Figures 3B and S2). Incubations amended with GO exhibited measurable enrichment of $^{13}CO_2$ after 2 days of incubation starting at the 2–5 cm core depth interval. The highest GO-AOM rate was measured at the 20–25 cm depth interval of 16.9 ± 2.3 ‰ day^{-1} $g_{DW}{}^{-1}$. Sediment with no additional electron acceptors exhibited an AOM rate that was the second highest for the 10–15 cm depth interval of 8.4‰ day^{-1} $g_{DW}{}^{-1}$, indicating the presence of residual, endogenous electron acceptors such as NOM or $SO_4{}^{2-}$. Incubations with ferrihydrite and $SO_4{}^{2-}$ did not lead to higher rates of AOM than the untreated sediment. The 16S rRNA gene sequencing results revealed that either *Methanoperedenaceae* or ANME2a-2b archaeal methanotrophs are present in these, with the latter clade being more abundant with increasing core depth.

Isotope measurements of porewater CH_4 revealed an enrichment in ^{13}C up to −49.3‰ and D up to +134.4‰ between 20 and 5 cm sediment depth (Figure 4C,D). Enrichment of heavy isotopes is considered a consequence of biological CH_4 oxidation, where the light isotopologue $^{12}CH_4$ is preferentially consumed compared with $^{13}CH_4$ and $^{12}CH_3D$ (Whiticar, 1999), but enrichments in δD up to +100‰ are rarely reported. Jacques et al. (2021), reported similarly high δD values in dissolved CH_4 in the Dutch Scheldt estuary and attributed them to oxidation. Additionally, we calculated the isotopic fractionation constants (Figure 4A,B), yielding values of −6.5‰ and −81.4‰ for $^{13}CH_4$ and D, respectively. These values are consistent with biological oxidation of CH_4, albeit on the low range of what is reported in literature (Milkov & Etiope, 2018). Thus, AOM activity was observed in the canal sediment that required an uncharacterized electron acceptor.

DISCUSSION

Our study demonstrates that canals in Amsterdam are a source of atmospheric CH_4, in line with previous findings for several other (urban) canal networks (Herrero Ortega et al., 2019; Peacock et al., 2021). *In situ* flux measurements showed that only the Amstel River was a source of CO_2 (Table 1), possibly due to aerobic respiration of organic matter (OM) in the water column and the sediment. While the Amsterdam canals studied here emitted CH_4, the concentration of CH_4 in the top 1 cm of the sediment pore water was lower than that in the water column. This could be caused by losses during sampling or spatial variability. Furthermore, ebullitive fluxes of CO_2 and CH_4 can contribute greatly to overall greenhouse gas emissions (Aben et al., 2017), but were not quantified here. Further measurements are needed on a larger scale to adequately determine total canal greenhouse gas emissions.

We hypothesized that NO_3^- could be driving AOM in the urban canals, due to the presence of *Methanoperedenaceae* since they are known to perform NO_3^--dependent AOM (Haroon et al., 2013; Pelsma et al., 2022; Raghoebarsing et al., 2006). NO_3^- was not detectable below the first two centimetres of sediment, but *Methanoperedenaceae* were found in the Amstel sediment at high relative abundances (Figure 2C). Incubations of the Amstel and Zoutkeetsgracht sediment showed low AOM activity, however, indicating that *Methanoperedenaceae* were not reactivated in the incubation experiments (Figure S3B). Members of the *Methanoperedenaceae* family are known to be able to use Fe(III) and Mn(IV) as electron acceptor for methanotrophy (Cai et al., 2018; Leu et al., 2020). However, the amendment of canal sediment with ferrihydrite showed only a very low rate of $^{13}CO_2$ enrichment, suggesting that Fe(III) is not a major electron acceptor in the canal sediments.

Since 5 mM of SO_4^{2-} was measured at the Dijksgracht canal, SO_4^{2-}-AOM could drive the anaerobic removal of CH_4. Moreover, a shallow SMTZ was observed at this site with a peak in sulphide at 9 cm sediment depth and ANME2a-2b are present from 5 cm core depth on at a relative abundance of 5%. However, the highest rates of AOM (both endogenous and GO-AOM) were measured below the SMTZ and SO_4^{2-}-amended incubations did not differ from incubations with autoclaved sediment. OM can be mineralized anaerobically by SRB in the upper layers of the sediment. As can be deduced from the decrease in SO_4^{2-} and increase in dissolved ammonium with increasing sediment depth, we hypothesize that the majority of SO_4^{2-} is used by SRB before it can penetrate to layers where ANME are more active. The concentration of sulphide was low (<2 μM), but the sediment Fe speciation shows the abundant presence of Fe(II), indicating that the sulphide produced is captured by sediment Fe, forming Fe monosulfide, and pyrite. The isotopic fractionation constants indicated biological removal of CH_4 in the sediment but are at the low end of values reported for known AOM processes (Milkov & Etiope, 2018; Whiticar, 1999). This may indicate that the observed methanotrophic activity is not related to the canonical SO_4^{2-}-AOM.

Our experiments showed that GO was the only alternative electron acceptor that exhibited higher rates of AOM compared with the endogenous control incubations. Microbial utilization of GO has been shown for five separate strains of *Shewanella* (Salas et al., 2010), the anammox bacterium *Ca*. Kuenenia (Shaw et al., 2020) and the anaerobic methanotroph *Ca*. Methanoperedens (Berger et al., 2021). When GO is reduced, it is converted to graphene, which is insoluble and precipitates. GO has the potential to act as a model molecule for NOM because it contains similar redox-active molecular structures, like quinone groups. NOM, previously referred to as humic substances, was implicated as a significant electron shuttle in coastal mangroves (Valenzuela et al., 2017) and paddy soils (Zhang et al., 2021). Valenzuela et al. (2017) reported on the stimulating effects of NOM on AOM. Similarly, Zhang et al. (2021) demonstrated that NOM addition can increase the efficiency of AOM. In both studies, the ANME2 clade of methanotrophic archaea were implicated to perform the observed AOM activity. In our experiments, ANME2a-2b were the most abundant anaerobic methanotrophs in the sediment layers where we observed that AOM was stimulated by the addition of GO. ANME2a-2b and *Methanoperedenaceae* are the two ANME clades that were detected in the sediment of the Dijksgracht. For ANME2 it was shown that in the presence of an organic electron acceptor they can oxidize CH_4 without a partner SRB (Scheller et al., 2016). *Methanoperedenaceae* were shown to be able to use NOM as electron acceptors by Bai et al. (2019) and *Ca*. Methanoperedens is able to oxidize CH_4 by donating electrons to an anode in a bioelectrochemical system (Ouboter et al., 2022; Ouboter et al., 2023). The relative abundance of ANME2a-2b increases with depth and is ∼20% in the core slices with the highest rates of AOM. Therefore, we have no indication that *Methanoperedenaceae* would be the main CH_4 oxidizers in the sediment. We suggest that in these canals AOM by ANME2 is decoupled from an SRB partner by the abundance of NOM present, allowing AOM activity to persist when SO_4^{2-} was depleted. Our solid phase analyses of the sediment supported this hypothesis as the sediments were rich in organic carbon (Figure S4). NOM-driven AOM has been shown in several ecosystems, such as rice paddy soils (Fan et al., 2020), marine anoxic waters (van Grinsven et al., 2020), mangrove soils (Sánchez-Carrillo et al., 2021), and anoxic lake sediments (Vigderovich et al., 2022). These data, combined with our results,

suggest that redox-active NOM may also act as the dominant electron acceptor for AOM in Amsterdam urban canals.

AOM has been described as a potential sink for CH_4 in sediments of freshwater lakes (Martinez-Cruz et al., 2018), streams (Shen et al., 2017), and in rice paddy soils (Fan et al., 2020). Parallels can be drawn between sediments from the Dijksgracht site and the Baltic Sea, since both are characterised by high OM input and brackish waters (Figure 2). In a study of estuaries sediments in Finland, for example, the highest AOM activity was observed in sediment layers below the SMTZ (Myllykangas et al., 2020), like the results reported in this study. The microbial community that was implicated for AOM was dominated by ANME2a-2b archaea. Furthermore, ANME2 archaea previously were suggested to oxidize CH_4 through AOM with SO_4^{2-} and Fe oxides in sediments of the brackish Bothnian Sea (Egger et al., 2015; Rasigraf et al., 2020). So far, no AOM mediated by NOM has been reported for Baltic Sea sediments. Future assays for AOM are advised to include treatments with NOM analogues to further assess their importance.

The shallow SMTZ that is described at the Dijksgracht site could be due to a relatively high rate of OM deposition in this canal. Such a shallow SMTZ is not unusual for eutrophic coastal systems (Van Helmond et al., 2020; Żygadłowska et al., 2023). The sediment at the Dijksgracht site indeed was also very rich in organic carbon (5 wt%) and SRB were detected in the top 10 cm of the sediment (Figures S2 and S3). In this setting, SO_4^{2-} reduction coupled to oxidation of OM appears to explain most of the SO_4^{2-} removal. Canonical marine SO_4^{2-} AOM typically dominates in sediments where SO_4^{2-} is more persistent due to lower organic carbon loading (Knittel & Boetius, 2009). We conclude that the urban OM at the Dijksgracht site is likely quite easily degradable, possibly as a result of anthropogenic pollution.

CONCLUSION

In conclusion, the results suggest that anaerobic methanotrophs and AOM activity were present in Amsterdam's canals. However, AOM did not capture all the CH_4 as we measured a CH_4 flux to the atmosphere at all tested sites. We found strong indications that NOM may act as an important electron acceptor in urban sediments. Because the ANME2a-2b implicated in AOM may rely on NOM as electron acceptor only, enrichments of these archaea could provide insight into an important environmental CH_4 filter.

AUTHOR CONTRIBUTIONS

Koen A. J. Pelsma: Conceptualization (equal); data curation (lead); formal analysis (lead); investigation (lead); methodology (equal); project administration (supporting); resources (supporting); software (lead); writing—original draft (lead); writing—review and editing (lead). **Niels A. G. M. van Helmond:** Conceptualization (supporting); data curation (supporting); investigation (supporting); methodology (equal); visualization (supporting); writing—original draft (supporting); writing—review and editing (supporting). **Wytze K. Lenstra:** Conceptualization (supporting); data curation (supporting); investigation (supporting); methodology (equal); visualization (supporting); writing—review and editing (supporting). **Thomas Roeckmann:** Data curation (supporting); methodology (supporting); writing—review and editing (supporting). **Mike S. M. Jetten:** Conceptualization (equal); project administration (equal); resources (equal); supervision (supporting); writing—original draft (supporting); writing—review and editing (supporting). **Caroline P. Slomp:** Conceptualization (supporting); writing—original draft (supporting); writing—review and editing (supporting). **Cornelia U. Welte:** Conceptualization (equal); project administration (equal); resources (equal); supervision (lead); writing—original draft (supporting); writing—review and editing (supporting).

ACKNOWLEDGEMENTS

The authors thankfully acknowledge funding from the NESSC gravitation program (grant no. 024002001) and the SIAM gravitation program (grant no. 024002002) granted by the Netherlands Organization for Scientific Research and the Ministry of Education, Culture and Science. This work was also supported by the European Research Council (ERC) Synergy Grant MARIX 854088. The authors would like to thank Waternet for sampling permission of the central canals. We thank Carina van der Veen of Utrecht University for help in measuring the methane isotopes. John Visser is thanked for measuring pore water NO_3^- and NO_2^- concentrations, Thom Claessen for measuring pore water SO_4^{2-}, Desmond Eefting for CN analysis and Helen de Waard and Coen Mulder for ICP-OES analysis of pore waters and sediment extracts.

CONFLICT OF INTEREST STATEMENT

The authors declare no conflict of interest.

DATA AVAILABILITY STATEMENT

All data in this study are deposited in public repositories of European Nucleotide Archive (https://www.ebi.ac.uk/ena/browser/view/PRJEB60458) and Zenodo (https://doi.org/10.5281/zenodo.7763073).

ORCID

Koen A. J. Pelsma https://orcid.org/0000-0003-3746-6528

Cornelia U. Welte https://orcid.org/0000-0002-1568-8878

REFERENCES

Aben, R.C.H., Barros, N., van Donk, E., Frenken, T., Hilt, S., Kazanjian, G. et al. (2017) Cross continental increase in methane ebullition under climate change. *Nature Communications*, 8(1), 1682.

Alshboul, Z., Encinas-Fernández, J., Hofmann, H. & Lorke, A. (2016) Export of dissolved methane and carbon dioxide with effluents from municipal wastewater treatment plants. *Environmental Science & Technology*, 50(11), 5555–5563.

Bai, Y.N., Wang, X.N., Wu, J., Lu, Y.Z., Fu, L., Zhang, F. et al. (2019) Humic substances as electron acceptors for anaerobic oxidation of methane driven by ANME-2d. *Water Research*, 164, 114935.

Berger, S., Shaw, D., Berben, T., Ouboter, H., Frank, J. & Welte, C. (2021) Current production by non-methanotrophic bacteria enriched from an anaerobic methane-oxidizing microbial community. *Biofilms*, 3, 100054.

Borges, A., Darchambeau, F., Lambert, T., Bouillon, S., Morana, C., Brouyère, S. et al. (2018) Effects of agricultural land use on fluvial carbon dioxide, methane and nitrous oxide concentrations in a large European river, the Meuse (Belgium). *Science of the Total Environment*, 610-611, 342–355.

Brigham, B.A., Bird, J.A., Juhl, A.R., Zappa, C.J., Montero, A.D. & O'Mullan, G.D. (2019) Anthropogenic inputs from a coastal megacity are linked to greenhouse gas concentrations in the surrounding estuary. *Limnology and Oceanography*, 64(6), 2497–2511.

Burdige, D. (2007) *Geochemistry of marine sediments*. Princeton: Princeton University Press.

Cai, C., Leu, A.O., Xie, G.-J., Guo, J., Feng, Y., Zhao, J.-X. et al. (2018) A methanotrophic archaeon couples anaerobic oxidation of methane to Fe(III) reduction. *The ISME Journal*, 12(8), 1929–1939.

Caporaso, J.G., Lauber, C.L., Walters, W.A., Berg-Lyons, D., Huntley, J., Fierer, N. et al. (2012) Ultra-high-throughput microbial community analysis on the illumina hiseq and miseq platforms. *The ISME Journal*, 6(8), 1621–1624.

Connor, N.P., Sarraino, S., Frantz, D.E., Bushaw-Newton, K. & MacAvoy, S.E. (2014) Geochemical characteristics of an urban river: influences of an anthropogenic landscape. *Applied Geochemistry*, 47, 209–216.

Conrad, R. (2009) The global methane cycle: recent advances in understanding the microbial processes involved. *Environmental Microbiology Reports*, 1(5), 285–292.

Dean, J.F., Middelburg, J.J., Röckmann, T., Aerts, R., Blauw, L.G., Egger, M. et al. (2018) Methane feedbacks to the global climate system in a warmer world. *Reviews of Geophysics*, 56(1), 207–250.

Egger, M., Rasigraf, O., Sapart, C.J., Jilbert, T., Jetten, M.S.M., Röckmann, T. et al. (2015) Iron-mediated anaerobic oxidation of methane in brackish coastal sediments. *Environmental Science & Technology*, 49(1), 277–283.

Ettwig, K.F., Zhu, B., Speth, D., Keltjens, J.T., Jetten, M.S.M., & Kartal, B. (2016). Archaea catalyze iron-dependent anaerobic oxidation of methane. *Proceedings of the National Academy of Sciences*, 113(45), 12792–12796.

Fan, L., Dippold, M.A., Ge, T., Wu, J., Thiel, V., Kuzyakov, Y. et al. (2020) Anaerobic oxidation of methane in paddy soil: role of electron acceptors and fertilization in mitigating CH_4 fluxes. *Soil Biology and Biochemistry*, 141, 107685.

Gao, Y., Wang, Y., Lee, H.-S. & Jin, P. (2022) Significance of anaerobic oxidation of methane (AOM) in mitigating methane emission from major natural and anthropogenic sources: a review of AOM rates in recent publications. *Environmental Science: Advances*, 1, 401–425.

Gessner, M., Hinkelmann, R., Nützmann, G., Jekel, M., Singer, G., Lewandowski, J. et al. (2014) Urban water interfaces. *Journal of Hydrology*, 514, 226–232.

Google Earth, (n.d.). [Google Earth satellite image of Amsterdam city centre]. https://earth.google.com/web/@52.37004883,4.90389332,5.06132473a,7970.06662902d,35y,1.62075033h,0.14649431t,0r

Haroon, M.F., Hu, S., Shi, Y., Imelfort, M., Keller, J., Hugenholtz, P. et al. (2013) Anaerobic oxidation of methane coupled to nitrate reduction in a novel archaeal lineage. *Nature*, 500(7464), 567–570.

Herlemann, D.P., Labrenz, M., Jürgens, K., Bertilsson, S., Waniek, J.J. & Andersson, A.F. (2011) Transitions in bacterial communities along the 2000km salinity gradient of the Baltic Sea. *The ISME Journal*, 5(10), 1571–1579.

Herrero Ortega, S., González-Quijano, C.R., Casper, P., Singer, G.A. & Gessner, M.O. (2019) Methane emissions from contrasting urban freshwaters: rates, drivers, and a whole-city footprint. *Global Change Biology*, 25, 4234–4243.

Hu, J., Ke, X., Wang, B., Mei, Y., Xiao, N., Wan, X. et al. (2022) SSThe coexistence and diversity of *Candidatus* methylomirabilis oxyfera-like and anammox bacteria in sediments of an urban eutrophic lake. *International Microbiology*, 25, 457–469.

Jacques, C., Gkritzalis, T., Tison, J.L., Hartley, T., van der Veen, C., Röckmann, T. et al. (2021) Carbon and hydrogen isotope signatures of dissolved methane in the Scheldt estuary. *Estuaries and Coasts*, 44, 137–146.

Knittel, K. & Boetius, A. (2009) Anaerobic oxidation of methane: Progress with an unknown process. *Annual Review of Microbiology*, 63(1), 311–334.

Lenstra, W., Klomp, R., Molema, F., Behrends, T. & Slomp, C. (2021) A sequential extraction procedure for particulate manganese and its application to coastal marine sediments. *Chemical Geology*, 584, 120538.

Leu, A.O., Cai, C., McIlroy, S.J., Southam, G., Orphan, V.J., Yuan, Z. et al. (2020) Anaerobic methane oxidation coupled to manganese reduction by members of the Methanoperedenaceae. *The ISME Journal*, 14(4), 1030–1041.

Marescaux, A., Thieu, V. & Garnier, J. (2018) Carbon dioxide, methane and nitrous oxide emissions from the human-impacted seine watershed in France. *Science of the Total Environment*, 643, 247–259.

Martinez-Cruz, K., Sepulveda-Jauregui, A., Casper, P., Anthony, K.W., Smemo, K.A. & Thalasso, F. (2018) Ubiquitous and significant anaerobic oxidation of methane in freshwater lake sediments. *Water Research*, 144, 332–340.

Milkov, A.V. & Etiope, G. (2018) Revised genetic diagrams for natural gases based on a global dataset of >20,000 samples. *Organic Geochemistry*, 125, 109–120.

Myhre, G., Shindell, D., Bréon, F.-M., Collins, W., Fuglestvedt, J., Huang, J. et al. (2013) Anthropogenic and natural radiative forcing. In: Stocker, T., Qin, D., Plattner, G.-K., Tignor, M., Allen, S.-K., Boschung, J. et al. (Eds.) *Climate change 2013: the physical science basis. Contribution of working group I to the fifth assessment report of the intergovernmental panel on climate change*. Cambridge, UK and New York: Cambridge University Press.

Myllykangas, J.-P., Rissanen, A.J., Hietanen, S. & Jilbert, T. (2020) Influence of electron acceptor availability and microbial community structure on sedimentary methane oxidation in a boreal estuary. *Biogeochemistry*, 148(3), 291–309.

Nisbet, E.G., Manning, M.R., Dlugokencky, E.J., Fisher, R.E., Lowry, D., Michel, S.E. et al. (2019) Very strong atmospheric methane growth in the 4 years 2014–2017: implications for the Paris agreement. *Global Biogeochemical Cycles*, 33(3), 318–342.

Ouboter, H.T., Berben, T., Berger, S., Jetten, M.S., Sleutels, T., ter Heijne, A. et al. (2022) Methane-dependent extracellular electron transfer at the bioanode by the anaerobic archaeal Methanotroph "Candidatus Methanoperedens". *Frontiers in Microbiology*, 13, 820989.

Ouboter, H.T., Mesman, R., Sleutels, T., Postma, J., Wissink, M., Jetten, M.S.M. et al. (2023) Mechanisms of extracellular electron transfer in anaerobic methanotrophic archaea. BioRxiv, Cold Spring Harbor Laboratory.

Peacock, M., Audet, J., Bastviken, D., Futter, M.N., Gauci, V., Grinham, A.R. et al. (2021) Global importance of methane emissions from drainage ditches and canals. *Environmental Research Letters*, 16, 044010.

Pelsma, K.A.J., In't Zandt, M.H., Op den Camp, H.J.M., Jetten, M.S.M., Dean, J.F. & Welte, C.U. (2022) Amsterdam urban canals contain novel niches for methane-cycling microorganisms. *Environmental Microbiology*, 24(1), 82–97.

Raghoebarsing, A.A., Pol, A., van de Pas-Schoonen, K.T., Smolders, A.J.P., Ettwig, K.F., Rijpstra, W.I.C. et al. (2006) A microbial consortium couples anaerobic methane oxidation to denitrification. *Nature*, 440(7086), 918–921.

Rasigraf, O., van Helmond, N.A.G.M., Frank, J., Lenstra, W.K., Egger, M., Slomp, C.P. et al. (2020) Microbial community composition and functional potential in Bothnian Sea sediments is linked to Fe and S dynamics and the quality of organic matter. *Limnology and Oceanography*, 65(S1), S113–S133.

Reeburgh, W.S. (2007) Oceanic methane biogeochemistry. *Chemical Reviews*, 107(2), 486–513.

Rosentreter, J.A., Borges, A.V., Deemer, B.R., Holgerson, M.A., Liu, S., Song, C. et al. (2021) Half of global methane emissions come from highly variable aquatic ecosystem sources. *Nature Geoscience*, 14(4), 225–230.

Salas, E.C., Sun, Z., Lüttge, A. & Tour, J.M. (2010) Reduction of graphene oxide via bacterial respiration. *ACS Nano*, 4(8), 4852–4856.

Sánchez-Carrillo, S., Garatuza-Payan, J., Sánchez-Andrés, R., Cervantes, F.J., Bartolomé, M.C., Merino-Ibarra, M. et al. (2021) Methane production and oxidation in mangrove soils assessed by stable isotope mass balances. *Water*, 13(13), 1867.

Saunois, M., Stavert, A.R., Poulter, B., Bousquet, P., Canadell, J.G., Jackson, R.B. et al. (2020) The global methane budget 2000–2017. *Earth System Science Data*, 12(3), 1561–1623.

Scheller, S., Yu, H., Chadwick, G.L., McGlynn, S.E. & Orphan, V.J. (2016) Artificial electron acceptors decouple archaeal methane oxidation from sulfate reduction. *Science*, 351(6274), 703–707.

Shaw, D.R., Ali, M., Katuri, K.P., Gralnick, J.A., Reimann, J., Mesman, R. et al. (2020) Extracellular electron transfer-dependent anaerobic oxidation of ammonium by anammox bacteria. *Nature Communications*, 11(1), 2058.

Shen, L., Ouyang, L., Zhu, Y. & Trimmer, M. (2019) Active pathways of anaerobic methane oxidation across contrasting riverbeds. *The ISME Journal*, 13(3), 752–766.

Shen, L., Wu, H.S., Liu, X. & Li, J. (2017) Cooccurrence and potential role of nitrite- and nitrate-dependent methanotrophs in freshwater marsh sediments. *Water Research*, 123, 162–172.

Takai, K. & Horikoshi, K. (2000) Rapid detection and quantification of members of the archaeal community by quantitative pcr using fluorogenic probes. *Applied and Environmental Microbiology*, 66(11), 5066–5072.

Valenzuela, E.I., Avendaño, K.A., Balagurusamy, N., Arriaga, S., Nieto-Delgado, C., Thalasso, F. et al. (2019) Electron shuttling mediated by humic substances fuels anaerobic methane oxidation and carbon burial in wetland sediments. *Science of the Total Environment*, 650, 2674–2684.

Valenzuela, E.I. & Cervantes, F.J. (2021) The role of humic substances in mitigating greenhouse gases emissions: current knowledge and research gaps. *Science of the Total Environment*, 750, 141677.

Valenzuela, E.I., Prieto-Davó, A., López-Lozano, N.E., Hernández-Eligio, A., Vega-Alvarado, L., Juárez, K. et al. (2017) Anaerobic methane oxidation driven by microbial reduction of natural organic matter in a tropical wetland. *Applied and Environmental Microbiology*, 83(11), e00645-17.

van Bergen, T.J.H.M., Barros, N., Mendonça, R., Aben, R.C.H., Althuizen, I.H.J., Huszar, V. et al. (2019) Seasonal and diel variation in greenhouse gas emissions from an urban pond and its major drivers. *Limnology and Oceanography*, 64, 2129–2139.

van Grinsven, S., Sinninghe Damsté, J.S. & Villanueva, L. (2020) Assessing the effect of humic substances and Fe (III) as potential electron acceptors for anaerobic methane oxidation in a marine anoxic system. *Microorganisms*, 8(9), 1288.

van Helmond, N.A.G.M., Robertson, E.K., Conley, D.J., Hermans, M., Humborg, C., Kubeneck, L.J. et al. (2020) Removal of phosphorus and nitrogen in sediments of the eutrophic Stockholm archipelago, Baltic Sea. *Biogeosciences*, 17, 2745–2766.

Vigderovich, H., Eckert, W., Elul, M., Rubin-Blum, M., Elvert, M. & Sivan, O. (2022) Long-term incubations provide insight into the mechanisms of anaerobic oxidation of methane in methanogenic lake sediments. *Biogeosciences*, 19(8), 2313–2331.

Wang, G., Xia, X., Liu, S., Zhang, L., Zhang, S., Wang, J. et al. (2021) Intense methane ebullition from urban inland waters and its significant contribution to greenhouse gas emissions. *Water Research*, 189, 116654.

Wang, X., He, Y., Chen, H., Yuan, X., Peng, C., Yue, J. et al. (2018) CH_4 concentrations and fluxes in a subtropical metropolitan river network: watershed urbanization impacts and environmental controls. *Science of the Total Environment*, 622-623, 1079–1089.

Whiticar, M.J. (1999) Carbon and hydrogen isotope systematics of bacterial formation and oxidation of methane. *Chemical Geology*, 161(1), 291–314.

Zhang, Y., Wang, F. & Jia, Z. (2021) Electron shuttles facilitate anaerobic methane oxidation coupled to nitrous oxide reduction in paddy soil. *Soil Biology and Biochemistry*, 153, 108091.

Żygadłowska, O.M., Venetz, J., Klomp, R., Lenstra, W.K., van Helmond, N.A.G.M., Röckmann, T. et al. (2023) Pathways of methane removal in the sediment and water column of a seasonally anoxic eutrophic marine basin. *Frontiers in Marine Science*, 10, 1085728.

SUPPORTING INFORMATION

Additional supporting information can be found online in the Supporting Information section at the end of this article.

How to cite this article: Pelsma, K.A.J., van Helmond, N.A.G.M., Lenstra, W.K., Röckmann, T., Jetten, M.S.M., Slomp, C.P. et al. (2023) Anaerobic methanotrophy is stimulated by graphene oxide in a brackish urban canal sediment. *Environmental Microbiology*, 25(12), 3104–3115. Available from: https://doi.org/10.1111/1462-2920.16501